Moderate ART resistance mutations with low fitness cost in malaria parasites from Africa

Hannah Michaela Behrens[1#], Sabine Schmidt[1#], Domitille Peigney[1], Jürgen May[2,3], Oumou Maïga-Ascofaré[2,3], Tobias Spielmann[1*]

[1]Malaria Cell Biology, Molecular Biology and Immunology, *Bernhard Nocht Institute for Tropical Medicine, Bernhard-Nocht-Str. 74, 20359 Hamburg, Germany.*

[2]Infectious Disease Epidemiology Department, Epidemiology and Diagnostics, *Bernhard Nocht Institute for Tropical Medicine, Bernhard-Nocht-Str. 74, 20359 Hamburg, Germany.*

[3]German Centre for Infection Research (DZIF), Partner Site Hamburg-Luebeck-Borstel-Riems, Hamburg, Germany

[#]equal contribution,

*corresponding author

Abstract

Combination therapies containing Artemisinin derivatives (ART) are the first line treatment of malaria but their effectiveness is reduced by resistance due to a fraction of ring stage *Plasmodium* parasites surviving high ART levels. Resistance-causing *kelch13* (*k13*) mutations are common in South East Asia but were only recently and sparsely detected in Africa, which experiences the highest malaria burden. Kelch13 shares a cellular compartment with other proteins (KICs) several of which cause resistance when inactivated or, in a few cases, when mutated. To see if the sparse detection of resistance mutations in Africa is due to unknown mutations, we tested 135 *k13* and *kic* mutations detected mostly in African field isolates. No *kic* mutation caused resistance but two in *k13*, V520A and V589I, did. These mutations were geographically much more widespread in Africa but conferred lower levels of resistance than known ART resistance mutations. A dissection of the mechanism using isogenic parasites with different *k13* mutations and parasites that we selected for even higher ART resistance, showed that resistance is a function of K13 protein levels in ring-stage parasites and correlates with the fitness cost. This indicated that hyper-resistance is unlikely to arise in the field. Double mutations in *k13* had not even additive effects and combinations including a non-*k13* mutation led to high fitness costs, suggesting that such combinations also pose no risk for higher resistance in the field. Overall, our results indicate that resistance is restricted by a proportional fitness cost but that incidence-lowering measures may favor high-resistance mutations.

Significance:

Our findings indicate that hyper-resistant parasites are unlikely to occur in endemic settings due to the proportional fitness cost. Mutations within *k13* were not additive and mutations outside *k13* had a disproportionally high fitness cost. The strong influence of the fitness cost may have favored moderate frequencies of the resistance mutations with low fitness cost detected in many African settings that we characterized in this study. These mutations, so far gone unnoticed, may be optimal in high endemicity regions, where relative drug use is presumably low but frequent multiple infections increase competition. A given endemic setting may thus favor variants with K13 levels for an optimal resistance-fitness balance which is relevant for incidence-lowering interventions.

Introduction

Malaria kills approximately half a million people per year, most of them children in sub-Saharan Africa (1, 2). Treatment heavily relies on artemisinin and its derivatives (ARTs) which are typically used in combination therapies (ACTs) with a partner drug (3). More than 10 years ago resistance to artemisinin was observed in low malaria incidence settings such as Asia, Oceania and South America. Resistance manifests as delayed parasite clearance after treatment, caused by some ring stage parasites surviving the ART-pulse, which is brief (1-2h) because of the low half-life of ART drugs. *In vitro* this resistance is measured by the ring stage survival assay (RSA) where survival of >1% of parasites indicates resistance (4).

The main cause of ART resistance are mutations in the *Pfkelch13* gene (*k13*) encoding the K13 protein (5, 6), which was recently found to be involved in endocytosis of host cell cytosol in the ring stage of the parasite (7). Ten mutations affecting the C-terminal propeller domain of K13 are confirmed to cause resistance as evident from delayed clearance (F446I, N458Y, M476I, Y493H, R539T, I543T, P553L, R561H, P574L, C580Y) and others have been associated with resistance (3).

Several other proteins, mostly from the K13-compartment, confer ART resistance in RSA either when downregulated or when mutated (7–11). Their contribution to resistance in the field is largely unknown.

Resistant clinical isolates and laboratory parasites carrying the resistance-associated mutations *k13* R539T and *k13* C580Y contain reduced amounts of K13 (7, 12–14). Artificially modulating K13 levels indicated that the reduced K13 levels lead to resistance (7, 12, 15). However, the impact of mutations on K13 levels and the relationship to resistance has not been systematically analysed and it is unclear whether other *k13* mutations confer resistance through the same mechanism or affect the functionality of K13.

While ART-resistance mutations are frequent in South East Asia, up to 100% in some locations (16–18), they are rare in Africa (17, 19, 20). Six validated resistance-conferring *k13* mutations (M476I, P553L, R561H, P574L, C580Y and A675V) have occasionally been reported in African countries at moderate to low frequency of 4.1% or less (21–23). Two exceptions are the R561H mutation in Rwanda, which was reported more frequently since 2019, most recently up to 16% (24–26) and the 11% of A675V mutation in Uganda in 2019 (23). It is not clear whether further resistance mutations exist in Africa that have not been studied yet because most studies focused on mutations occurring in Asia and systematic *k13* surveillance is still lacking in Africa. In agreement with the rare occurrence of resistance mutations, treatment failure occurs at less than 1% in Africa (27), with the exception of the Masaka region in Rwanda at 16%, where *k13* R561H occurs (26). However, a high proportion of immunity and the high multiplicity of infections in the African population might hamper parasites surviving ART treatment in patients (28, 29).

The reduced endocytosis in ART resistant parasites results in an amino acid deprivation (30) and there is clear evidence for a fitness cost of ART resistance (6, 31). Usually considerably less than 50% of parasites from resistant patient isolates survive in the RSA (5) and the delayed clearance rather than full loss of susceptibility in patients could indicate that parasites with higher levels of ART resistance might arise. However, it is at present unclear if and to what extent the fitness cost impedes higher levels of resistance in endemic areas. It is also unclear if combinations of mutations could lead to hyper-resistant parasites.

Here we report that two *k13* mutations which are present in parasites from several African countries (32, 33) afford moderate but significant resistance to ART. We show that these mutations incur a much smaller fitness cost than the C580Y mutation, the most common mutation in South East Asia. A

comparison of parasites with these and other mutations shows a correlation between resistance, fitness cost and K13 protein abundance of a given variant, suggesting a strong constraint of resistance levels by the fitness cost. This was confirmed by parasites artificially selected for higher resistance. High endemicity settings, typical for many African regions, are characterized by frequent multiple infections and likely infrequent ACT use due to partial immunity (34–36). Our work raises the possibility that this resulted in a selection pressure favoring low level resistance to ART and that this may be a reason for the differences in the geographic distribution of *k13*-mutations. This may be of relevance for interventions reducing malaria burden. Our results also indicate that the fitness cost may prevent the occurrence of hyper-resistant parasites with the K13-based mechanism unless other changes evolve in the parasite that counter act the fitness cost. Finally, we find no evidence for increased resistance in parasites with double mutations or mutations outside *k13* and these may therefore not pose a threat for hyper-resistance.

Results

Low-prevalence *k13* mutations found in Africa cause ART resistance

We hypothesized that in a holoendemic region such as Africa mutations causing resistance could only be present at low to moderate prevalences (< 5%) or confer only limited resistance as otherwise wide-spread treatment failure would already have been observed. In addition, we took into consideration that not only *k13*, but also genes of K13 compartment proteins such as *ubp1* could be mutated. We therefore decided to analyze non-synonymous mutations in *k13* and genes of other K13 compartment proteins with low to medium prevalence in patient samples from Africa based on the data available from WWARN (37), the Ghanaian Fever Without Source study (38) and MalariaGen (39). These included mutations in the genes encoding K13, KIC1, KIC2, KIC4, KIC5, KIC7, KIC9, UBP1, EPS15, AP-2α and MyoF (previously annotated as MyoC) (list of mutations in Table S1). Due to the large number of mutations in the K13 compartment proteins (a total of 131 mutations in ten genes) we created mutation pools by simultaneously introducing several mutations into the same gene in 3D7 parasites using selection-linked integration (SLI, (40)) (Table S1). In total 125 mutations were included in 8 mutation pools and 6 mutations were tested individually. RSAs (using dihydroartemisinin (DHA)) with the parasites harboring the pools of mutations in compartment members of K13, showed no change in susceptibility to ART, suggesting that none of the mutations in the genes encoding KIC1, KIC2, KIC4, KIC5, KIC7, KIC9, UBP1, EPS15, AP-2α and MyoF resulted in ART resistance (Figure 1A and Figure S1).

For *k13* itself we chose the mutations V520A, V589I and E612K that have been found with low to moderate prevalence in different malaria endemic regions in Africa and were not previously tested for ART resistance *in vitro* (32, 33, 41). E612K was found only in Cameroon with a prevalence of 0.8% in 2016. The prevalence of the other mutations was between 1.3% in Ghana in 2012 and 4.0% in the Democratic Republic of Congo in 2007 for V520A, and between 0.3% and 5.0% in Equatorial Guinea for V589I in 2018 and 2013, respectively (Figure 1B and Dataset S1). All samples analyzed in the 35 studies that detected these three mutations were taken after ACT started to be used in the respective country, with exception of one study in Kenya in 2002 (Dataset S1).

The respective mutations were introduced into the *k13* locus of *P. falciparum* 3D7 parasites together with GFP to result in a GFP-K13 fusion as done previously (7) and the susceptibility to ART was tested by RSA. *k13* V520A resulted in 1.1% (±0.4%) mean survival and V589I in 1.9% (±1.2%) mean survival, therefore both were above the threshold for resistance (1% survival (42)), whereas E612K (0.6% mean survival) did not render parasites resistant to ART (Figure 1C). This is in agreement with previous observations that mutations conferring resistance to ART occur in the K13 propeller domain but not in the fourth and fifth blade (residues 581 to 666) of this propeller (43). In conclusion, *k13* mutations

resulting in moderate ART-resistance when tested in a laboratory isolate are widespread on the African continent at moderate to low prevalence.

For comparison, we also tested *k13* C580Y, R561H and R539T, which were previously shown to be resistance mutations and *k13* E252Q, which occurred in Thailand and Myanmar between 2005 and 2013 where it was previously associated with slow clearance but not tested *in vitro*. This latter mutation was also of interest because it is not in the Kelch propeller domain. Similar to V520A and V589I, E252Q conferred a moderate level of resistance in RSA (1.0% (±0.6%)), while the known resistance mutations C580Y (16.3% ±6.1%), R561H (11.1% ±8.0%) and R539T (38.4% ±13.2%) showed higher proportions of surviving parasites (Figure 1C), similar to what was previously observed for C580Y and R539T in 3D7 (5). E252Q is unusual in that it confers resistance despite being situated in the N-terminal domains of K13 instead of its propeller domain. Of note, a non-propeller domain mutation, *k13* P413A, was recently found to also confer resistance but this mutation is located in the BTB/POZ domain that in contrast to the region of the E252Q mutation is still part of K13 conserved with proteins in other organisms (44).

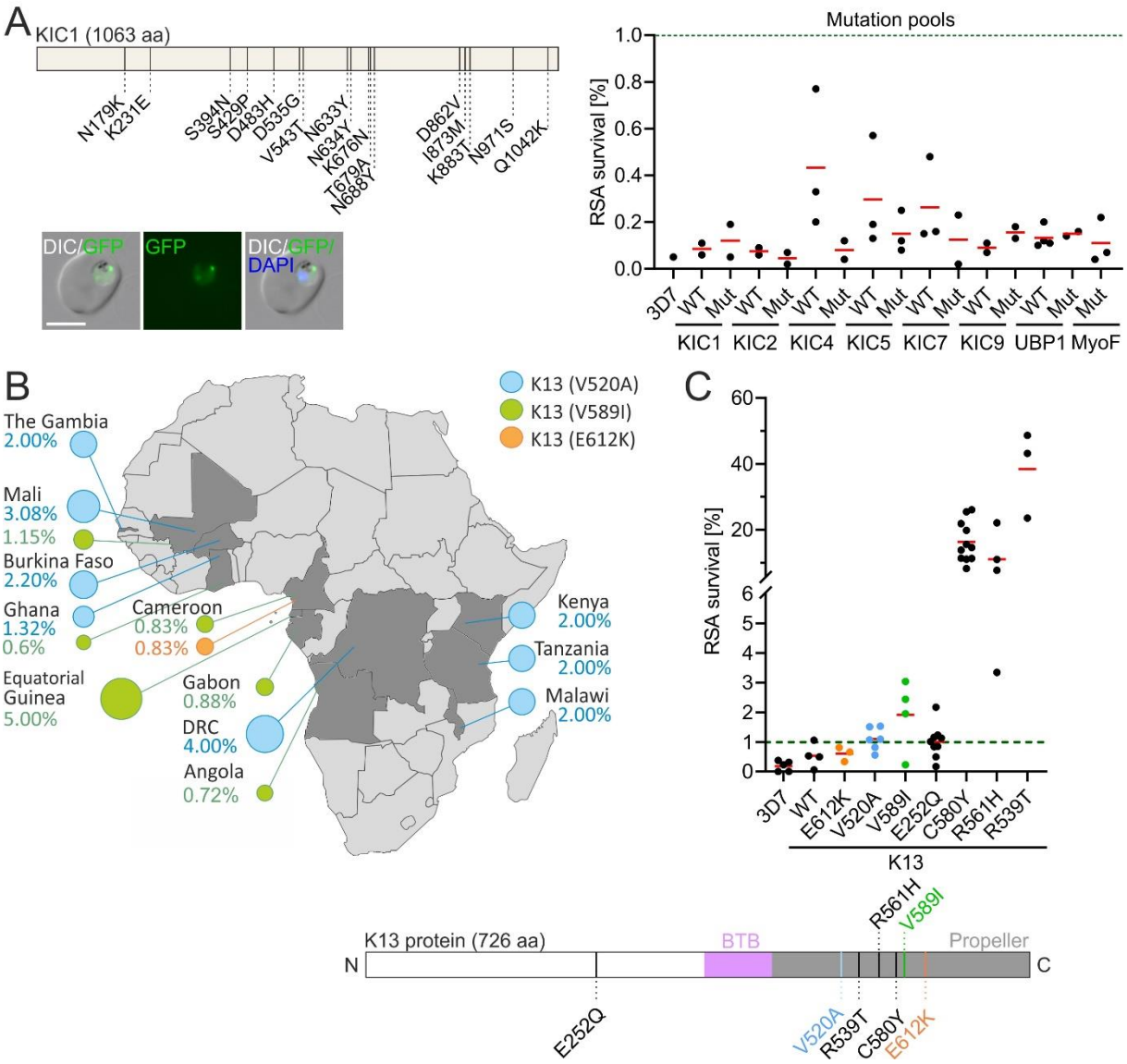

Figure 1: Low prevalence mutations cause moderate levels of ART resistance. (A) Mutations introduced in the mutation pool of KIC1 are exemplarily shown in a schematic and fluorescence images of the resulting parasites harboring KIC1 with all pool mutations are shown. Scale bar 5 µm. RSA survival for all mutation pools is displayed (% survival compared to control without DHA 66 h after 6 h DHA treatment in standard RSA). (B) Map of Africa illustrating geographical distribution of mutations and corresponding prevalence. Highest mutation frequency detected in each country is shown. Circle area is

proportional to prevalence. DRC, Democratic Republic of the Congo. (C) RSA of different K13 mutant cell lines. WT, wild type; red bars indicate the mean parasite survival rate of the respective cell line, each dot represents an independent experiment, green dashed line represents the 1% cut-off value defining parasites resistant to ART. Position of *k13* mutations is shown on K13.

Double mutations in *k13* do not significantly increase ART resistance

To anticipate how *k13* resistance phenotypes could further develop in endemic areas, we investigated whether the combination of the *k13* C580Y mutation (which is highly prevalent in SE Asia) with the newly identified low-resistance mutation V520A or the known high-resistance mutation R539T poses the risk of hyper-resistance. To obtain the corresponding cell lines, we again modified the endogenous *kelch13* locus of 3D7 parasites using SLI so that the double mutated K13 was also fused to GFP. The $K13^{V520A+C580Y}$ parasites did not display an increased resistance level in RSAs compared with parasites with only the C580Y mutation (16.3% mean survival) but showed a non-significant decrease (11.5% survival) (Figure 2A). Similarly, $K13^{R539T+C580Y}$ parasites showed non-significantly decreased RSA survival (33% survival) compared with parasites with R539T alone (38% survival) but significantly more survival than the C580Y alone. In conclusion, the combination of a low- and a high-resistance mutation or two high-resistance mutations—at least with the tested mutations—is neither additive nor synergistic.

Selection by consecutive RSAs significantly increases ART resistance

In a further attempt to anticipate increased resistance, we tested whether resistant parasites can be selected for increased resistance by performing consecutive RSAs. For this, an RSA was carried out with $K13^{C580Y}$ parasites and surviving parasites were subjected to another RSA as soon as they reached sufficient parasitemia following the previous RSA (Figure 2B). After 29 iterations of RSAs, we obtained the parasite line $K13^{C580Y}$-29^{th}. These parasites displayed significantly increased survival in RSA (39.2% mean survival) compared with the original $K13^{C580Y}$ parasites at the start of this experiment (12.4% mean survival) (Figure 2C), showing that repeated ART-treatment of *k13* C580Y-harbouring parasites can increase ART resistance. Sequencing of *k13* in these parasites showed that this was not due to additional *k13* mutations apart from C580Y.

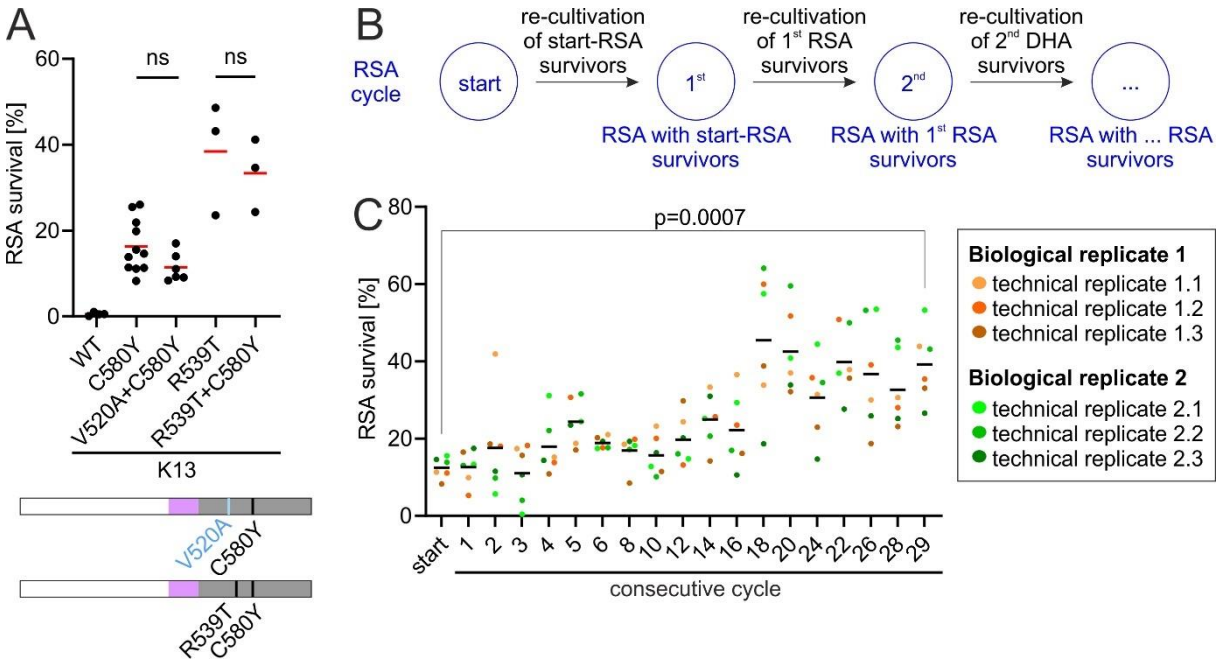

Figure 2: DHA-selection but not combination of low and high resistance mutations increases resistance. (A) RSA of the different *k13* mutant cell lines indicated. WT, wild type; each point represents an independent RSA; red bars indicate the mean parasite survival rate of the respective cell line. Position of *k13* mutations are shown on K13. Domains are colored as in figure 1. (B) Scheme of experimental procedure of consecutive standard RSA cycles performed with DHA survivors of the respective prior cycle. (C) Parasite survival rate of $K13^{C580Y}$ (% survival compared to control without DHA) 66 h after 6 h DHA treatment in standard RSA. Six experiments per cycle were performed, consisting of two biological and three technical replicates (see color code). P value is indicated, two-tailed Student's t-test. Red bars show mean.

Cellular levels of K13 and KIC7 determine ART-resistance

Previously, we and others showed that the level of K13 in the $K13^{C580Y}$ parasites is lower than in $K13^{wt}$ parasites and that reducing K13 abundance resulted in resistance (7, 12). We therefore assessed the cellular K13 levels in the parasites with the V520A and V589I mutations. We previously used either Western blots or direct microscopy-based measurement of GFP fluorescence in the cells to determine K13 levels (7). Here we used direct microscopy-based measurement of K13 levels because in comparison to Western blots, which are only semi-quantitative, this procedure is not susceptible to influence of cell lysis and the multiple steps required for blotting and detection. These experiments showed that the level of K13 with the V520A mutation was 94% of WT K13 level and K13 with V589I was 92% of WT (Figure 3A). This reduction in protein levels was more modest than observed for the high-resistance mutations *k13* C580Y, *k13* R561H and *k13* R539T which showed 52%, 51% and 51% compared with WT, respectively (Figure 3A). As expected from their RSA resistance behavior, parasites with the *k13* V520A C580Y double mutation harbored similar levels of K13 as parasites with the *k13* C580Y alone (48% of WT), while the K13 levels in $K13^{C580Y}$-29^{th} parasites showed a further reduction (32% of WT) when compared with $K13^{C580Y}$ parasites (Figure 3A and S2). The E252Q mutation showed no reduction (105% of WT). Differences between WT and K13 harboring R561H, R539T or C580Y with or without other mutations were significant comparing the means (Figure 3A) or individual values (Figure S2). Given the small differences between WT and V520A, V589I or E252Q, obtaining statistically backed results would be difficult, but it can be concluded that there is either a small or no reduction of the abundance of V520A and V589I variants in in the cell.

We noted that high resistance mutations had low K13 levels and low resistance mutations had high K13 levels. To better explore this relationship, we plotted the cellular K13 levels against RSA survival (resistance) and found that cellular K13 levels correlated with resistance (Pearson's r=-0.81, p=0.005) (Figure 3B). The mutations clustered in two groups, one high resistance-low K13 levels group, including the C580Y mutation and a low resistance-high K13 levels group, including the V520A and V589I mutations.

To test whether RSA-resistance not just correlates with but is determined by the amount of K13 in its cellular location, we used K13 1xNLS parasites (7). In this line K13 protein is removed into the nucleus by a nuclear localization signal (NLS) upon addition of rapalog, resulting in a knock sideway. Previously, 250 nM rapalog was used to achieve a knock sideway of K13 (40). Here, we used different concentrations of rapalog to result in different levels of K13 protein remaining at its site of action. ART-resistance as measured by RSA increased as the rapalog concentration and hence K13 knock sideway increased, confirming that RSA-survival is a function of K13 levels in the parasites (Figure 3C). These results confirm observations made on parasites in which the K13 abundance was titrated on mRNA level through the glmS system and determined RSA survival rates (15). We performed a second titration on KIC7, a K13-compartment protein, which was also mislocalized using the same increasing rapalog concentrations as for K13 (Figure 3D). Again, RSA survival was dependent on the level of knock sideways of KIC7 (i.e. amount of KIC7 at the K13 compartment), indicating that the activity of the

endocytic process determines resistance and that this occurs through the available amount of the proteins involved in this process.

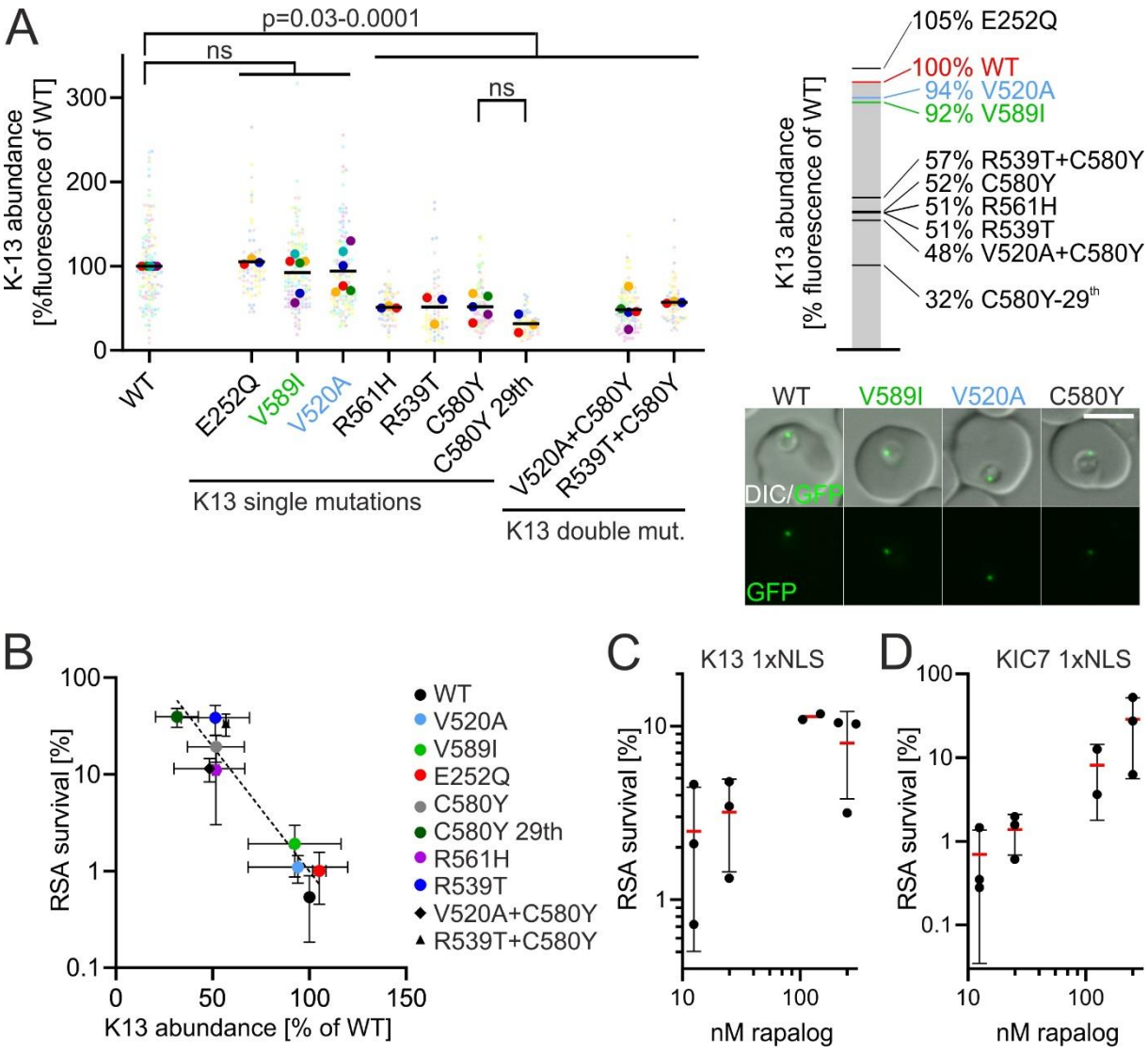

Figure 3: Resistance is inversely correlated with K13- and KIC7-abundance. (A) K13-abundance measured by the GFP fluorescence intensity of the single focus observed in ring stage parasites with the indicated K13 expressed from the endogenous locus and fused to GFP, normalized to the fluorescence in parasites with the identically modified endogenous locus but with a WT GFP-K13. Each small dot represents the measured value from one focus in one parasite. Large dots of the same color as small dots represent mean of the respective measured values and each large dot represents one biological replicate. P-values derive from comparing means by one-way ANOVA. Example fluorescence microscopy images are shown. Scale bar 5 µm. (B) Mean of parasite survival in standard RSA plotted against mean of K13-abundance. Error bars show standard deviations. (C) RSA survival of K13 1xNLS parasites grown in the presence of 12.5 nM, 25 nM, 125 nM or 250 nM rapalog for 3 h before and 6 h during the DHA exposure of the RSA. (D) RSA survival of KIC7 1xNLS parasites grown in the presence of 12.5 nM, 25 nM, 125 nM or 250 nM rapalog for 3h before and 6h during the DHA exposure of the RSA. Red bar, mean; standard deviation indicated; each dot derives from an independent experiment.

Fitness cost correlates with ART-resistance

In contrast to parasites harboring C580Y, parasites with *k13* V520A and V589I mutations are prevalent in Sub-Saharan African countries, with particularlyV520A showing a wide distribution (Figure 1B). This

raises the question whether high malaria prevalence, such as in Sub-Saharan Africa, favors parasites with a low resistance (compared with high resistance) due to a lower fitness cost of these mutations if no drug pressure is applied. Fitness cost might be critical in Africa because of the additional selection pressure from within-host competition which in turn results from high multiplicities of infections (36) and because of partial-immunity of the human population which might result in lower relative ART usage in the infected population (36). Several studies modelling fitness and within-host competition have highlighted the importance of fitness cost and propose that resistant parasites with high fitness cost are less likely to establish themselves in high transmission areas like Africa (29, 45, 46). Yet resistance mutations that confer low resistance and low fitness costs have not been considered in this context.

To measure fitness of the *k13* mutants, we first monitored *in vitro* growth after 96 h. $K13^{V520A}$ and $K13^{V589I}$ parasites showed no significant growth defect compared to $K13^{WT}$ (Figure 4A). In comparison, parasites harboring the C580Y mutation showed a significant growth defect as described before (18). When RSA survival was plotted against growth for each of the parasite lines with different *k13* mutations, the parasite lines clustered into two groups: one with low fitness and high resistance (all parasites harboring the *k13* C580Y mutation) and one with high fitness and low resistance (*k13* V520A and V589I), possibly reflecting different selection pressures in the different transmission settings (Figure 4B).

Previously, fitness costs of *k13* mutations have been measured by observing the growth of a mixed culture of a mutant and a parent parasite line (18, 47). To further investigate the fitness costs of the newly detected resistance mutations *k13* V520A and *k13* V589I the respective parasites were mixed 1:1 with 3D7 parasites and the proportion of mutated parasites was tracked until it made up less than 5% of the parasite population (Figure 4C and S3). For comparison, the same experiment was performed with $K13^{C580Y}$, $K13^{C580Y}$-29^{th} and $K13^{E252Q}$ parasites. Similar to what was observed when parasites growth was tracked in individual cultures, there was a trend that the RSA-survival caused by a mutation correlated with the fitness cost it inflicted (Figure 4D). However, this trend was not significant (Pearson's r=0.69, p=0.13) because *k13* V520A behaved as an outlier to the trend in half of the experimental repeats, in which its growth slowed severely after the start of the experiment (Figure S3), while in the other half it grew as expected from the trend of the other mutations (Pearson's r=0.90, p=0.04 when V520A was excluded) (Figure 4C). It is unclear why the *k13* V520A cell line grew much less than expected in some experiments but it is possible that independent factors impaired the growth of these parasites or that this mutation has effects differing from the other mutations but that these effects are not relevant at all times.

In conclusion, the level of ART-resistance a *k13* mutation causes correlates with its fitness cost (Figure 4A-D). Together with the findings on K13 abundance (Figure 3), it is therefore likely that both fitness cost and ART-resistance are caused by the reduced amount of K13 in the cell as a result of the destabilization of the K13 protein through the given mutation.

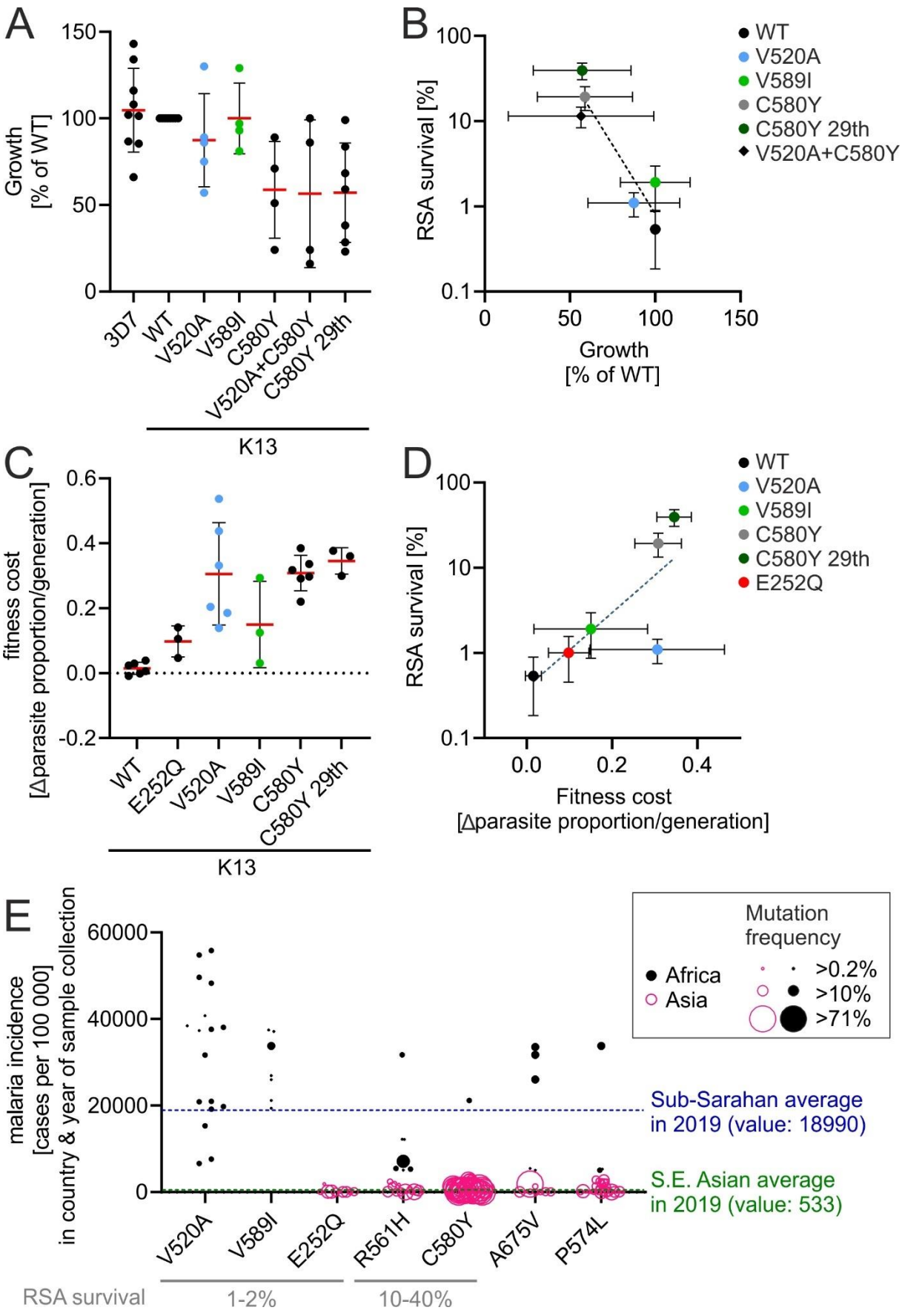

Figure 4 Fitness cost correlates with resistance: (A) Parasite growth, calculated as fold-change of parasitemia after 96 h compared to parasitemia at 0 h, normalized to WT growth for different cell lines with indicated *k13* mutations. (B) Mean of growth of strains harboring different *k13* mutations plotted against mean of parasite survival in RSA. Dashed line shows linear regression against log-transformed data. (C) Fitness cost of parasites harboring different *k13* mutations grown in competition

with 3D7 parasites given as loss of parasite proportion/generation. (D) Mean of fitness cost plotted against mean of parasite survival in RSA. All error bars show standard deviations. Black dashed line shows linear regression against log-transformed data. (E) Malaria incidence at place and time of *k13* resistance mutation detection. RSA survival shown as determined in this work (Figure 1B).

Following the hypothesis that the lower fitness cost of low-resistance mutations might be an advantage in areas with high malaria incidence because of the higher in-host competition and lower treatment frequency in the infected population, we compared the malaria incidence at which the different *k13* mutations occurred in Africa (black, Figure 4E, Dataset S2). As there is no continuous monitoring of *k13* mutations in most African countries, the comparison relied on individual studies that were conducted at different times and places (data from WWARN (48)). For each detection of a *k13* resistance mutation on the African continent, the malaria incidence in that country and year was plotted (data from IHME Burden Of Disease (49)). For comparison the occurrence of the same mutations in Asia was also added (pink, Figure 4E). For instance, *k13* V520A was detected in 17 studied populations in countries that had malaria incidences ranging from 6604 to 55829 malaria cases per 100000 inhabitants in the year of the detection of this mutation. The frequency of the V520A mutation among all sequenced samples ranged from 1.3% to 2.5% (circle area, Figure 4E). Like *k13* V520A, *k13* V589I was only detected in Africa. The other *k13* resistance mutations that were detected in Africa also occurred in Asia. Overall, the low-resistance mutations *k13* V520A and V589I occurred in regions with higher malaria incidence than the high resistance mutations R561H and C580Y (Figure 4E) and were detected in more study populations (Figure 4E) and in a wider geographical range than R561H and C580Y (Figure 1B). *k13* A675V and P574L were detected in low and high incidence areas, but their resistance level cannot be compared because it was not tested in isogenic backgrounds. E252Q was only detected in Asia, with all but one occurrence in Thailand where its frequency decreased as malaria incidence dropped (Figure S4). At the same time the frequency of C580Y increased, which supports that the high resistance mutation C580Y has a competitive advantage at low malaria incidence. Nonetheless, it is surprising that E252Q has not been observed in places with higher malaria incidence in Africa but this might be because often only the propeller domain is sequenced when screening for resistance mutations (Figure 4E).

ubp1 R3138H increases fitness cost but not ART resistance in K13^{C580Y} parasites

After assessing the effect of the *k13* double mutations V520A+C580Y and R539T+C580Y, we wondered whether there are combinations of mutations or gene disruptions beyond *k13* that harbour the risk of very high resistance levels. To test this we used parasites with *kic4* and *kic5* targeted gene disruptions (TGD), two lines previously shown to have increased parasite survival in RSA and a reduced growth (7). In addition we used parasites with the R3138H mutation in *ubp1* (encodes UBP1) which had been detected in patient isolates in SE Asia and confers moderate levels of ART-resistance in RSA (7, 50).

We aimed to generate three different parasite lines: parasites with *ubp1* R3138H and a disrupted *kic4*, parasites with *ubp1* R3138H and disrupted *kic5*, parasites with disrupted *kic4* and *kic5*. Six integration attempts using selection linked integration were done for each parasite line, with at least 14 weeks on the selection drug or until parasites reached at least 0.1% parasitemia, but no parasite lines with correct integration were obtained. Additionally, three attempts were made to generate the *kic4+kic5* double disruption parasite line by the reverse approach of disrupting *kic4* in *kic5*-TGD parasites, instead of *kic5* in *kic4*-TGD parasites, with at least 11 weeks on the selection drug or until parasites reached at least 0.1% parasitemia. Again, no parasite lines with the correct integration were obtained. Failure to obtain these lines indicates that the fitness cost of these combinations of gene disruptions and mutations may have been too high for the parasites to survive. Based on this, it seems that double mutations including the disruption of *kic4* or *kic5* (and possibly other K13 compartment proteins

affecting endocytosis and resistance) are not likely to contribute to the development of higher ART-resistance in the field.

Finally, we investigated the possibility of *k13* mutations combined with mutations in other proteins by combining *k13* C580Y with *ubp1* R3138H. We successfully introduced this combination, yet the resulting $K13^{C580Y}$+$UBP1^{R3138H}$ parasites did not display a significantly increased resistance level (17.3% mean survival) compared with parasites with the C580Y mutation alone (Figure 5A). As before (Figure 3B), the K13 abundance correlated with ART resistance as measured by RSA survival (Figure 5B and C). The growth of $K13^{C580Y}$+$UBP1^{R3138H}$ parasites was slower than that of $K13^{C580Y}$ parasites and $UBP1^{R3138H}$ parasites, which each confer a fitness cost, both when measured in individual cultures and direct competition assays (Figure 5D-G). Of particular note is that the *ubp1* R3138H mutation alone caused a disproportionally low growth compared to the level of ART resistance it affords when compared to all tested *k13* mutations (Figure 5E). This is congruent with our previous finding that in contrast to K13, UBP1 is also important for hemoglobin endocytosis in trophozoites (7) and could explain why we were not able to combine this mutation with *kic4* and *kic5* TGDs and why this mutation has rarely been observed in patient samples. Overall, due to its disproportionally high fitness cost and lacking synergism with *k13* mutations, *ubp1* R3138H and likely mutations in other K13 compartment proteins important for endocytosis in trophozoites are therefore not probable to combine with *k13* mutations in the field.

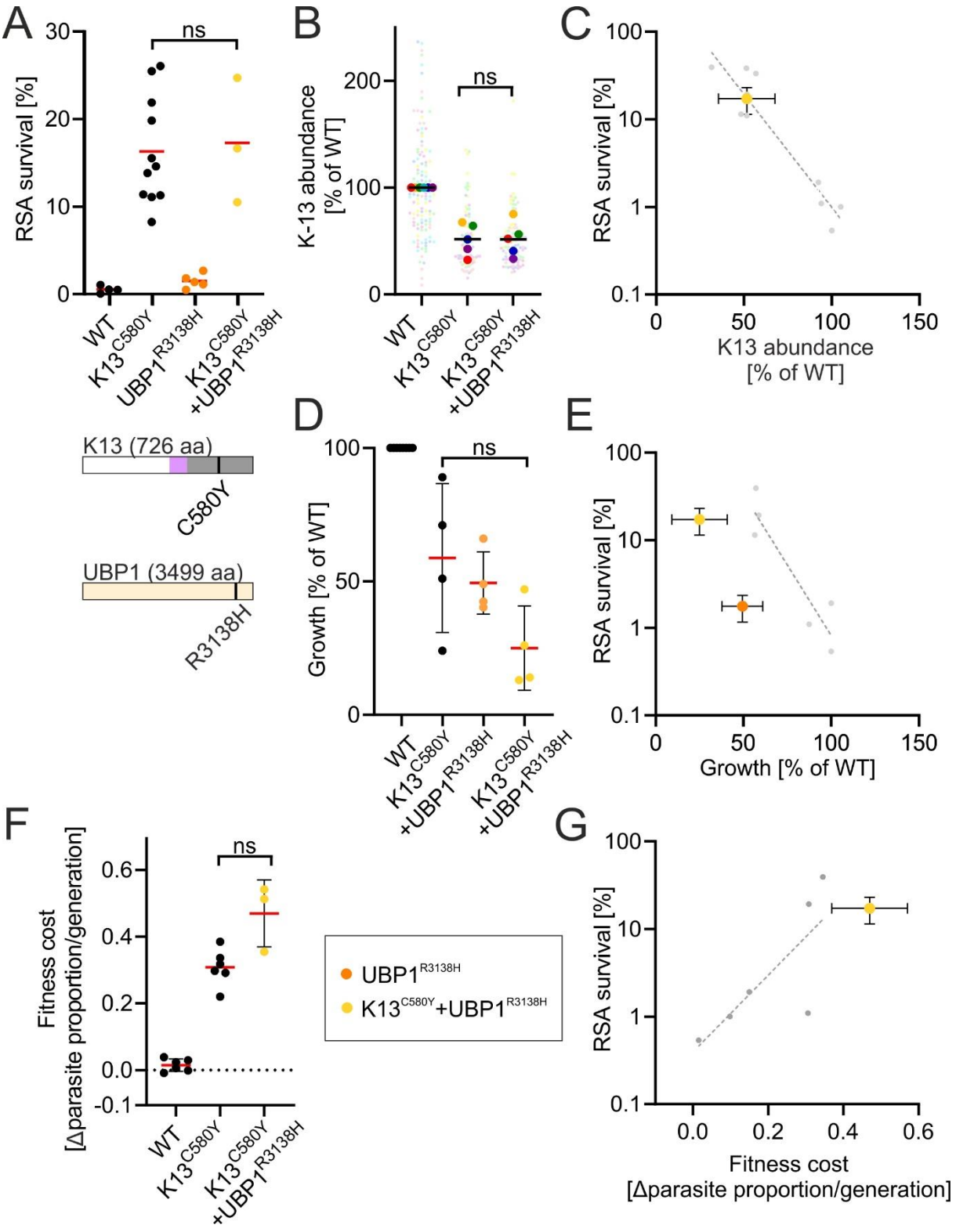

Figure 5: Double mutation of *k13* C580Y and *ubp1* R3138H result in a high fitness cost. (A) RSA of K13^{C580Y} and UBP1^{R3138H} single and double mutant cell lines. Red bars indicate the mean parasite survival rate of the respective cell line. Data for UBP1^{R3138H} was previously published in (7). Position of *k13* and *ubp1* mutation is depicted in K13 and UBP1. K13 domains are colored as in figure 1. (B) K13-abundance measured GFP fluorescence intensity of the single focus observed in ring stage parasites of the indicated K13 expressed from the endogenous locus and fused to GFP, normalized to the fluorescence in parasites with the identically modified endogenous locus but with a WT GFP-K13. Small dots represent measured values for individual parasites. Large dots of the same color as small dots represent mean of the respective measured values and each large dot represents one biological replicate. Dots of the same color were obtained as part of the same experimental repeat. (C) K13 abundance plotted against parasite survival in RSA for K13^{C580Y}+UBP1^{R3138H} parasites (yellow). Grey dots show data of *k13* mutations from Figure 3B. (D) Growth, calculated as fold-change of parasitemia after 96 h normalized compared to

parasitemia at 0 h for different cell lines with indicated *k13* or *ubp1* mutations. (E) Growth of strains harboring *ubp1* R3138H with (yellow) and without (orange) *k13* C580Y plotted against parasite survival in RSA. Grey dots show data of *k13* mutations from Figure 4B. (F) Fitness cost for different cell lines with indicated *k13* or *ubp1* mutations grown in mixed cultures with 3D7. (G) Fitness cost $K13^{C580Y}$+$UBP1^{R3138H}$ parasites (yellow) plotted against parasite survival in RSA. Grey dots show data of *k13* mutations from Figure 4D. All error bars show standard deviations.

Discussion

Based on our findings in this work we conclude that moderate-resistance mutations in *k13* may have been present in parasites from many African countries for several years. Due to their lower fitness cost, they may be favored in high malaria incidence settings due to high inter-parasite competition (high rate of multiple infections) and lower treatment rates in the infected population (34–36). Our findings therefore suggest that lowering malaria incidence through control measures may increase the risk for the development of higher level resistance, as previously proposed (27, 35, 43, 51, 52). The presence of low-resistance mutations in Sub-Saharan Africa also shows that resistance can occur at high malaria incidence. At the moderate mutation frequency, low resistance levels and remaining effective partner drugs this may not be immediately evident in patient care. However, it is crucial to closely monitor resistance mutations and treatment efficacy in Africa, especially during interventions that increase drug use to lower malaria incidence and may thus raise the equilibrium of resistance level that is stable in the parasite population.

ART resistance clearly correlated with K13 levels for all *k13* propeller domain-mutations tested, indicating that resistance is a function of K13 abundance. Hence, mutations that confer resistance likely destabilize K13. As artificially titrating K13 or KIC7 levels had a similar effect it can be inferred that this is due to a proportional reduction in endocytosis. The same effect on resistance was observed in a K13 titration recently (15) and the role of K13 protein abundance in resistance is also supported by the finding that increasing levels of K13 C580Y reverts resistant parasite back to sensitive (7). Interestingly, for E252Q, which is located outside the propeller domain, protein levels were not reduced. While the protein level differences for such moderate resistance mutations are too small for rigorous conclusions, it is nevertheless tempting to speculate that this mutation reduced K13 activity rather than protein levels. Interestingly, $K13^{C580Y}$-29^{th} parasites selected for higher resistance had even further reduced levels of K13 than $K13^{C580Y}$, confirming that K13 protein levels are a central determinant of ART resistance. By what mechanism the $K13^{C580Y}$-29^{th} strain achieved lower K13 levels (and hence higher resistance levels) is at present unclear but additional *k13* mutations were here excluded.

The finding that ART resistance correlated with fitness cost of the tested *k13* mutations agrees with a recent study looking at *k13* M579I, C580Y and R561H in several African strains including 3D7 although no such correlation was observed in the Asian strain Dd2 (18). It is unclear what caused these differences between African strains and Dd2. Nonetheless, it showed that the genetic background in which the mutations occur can influence the fitness cost and the resistance level (18, 31, 53). Many differences have been observed in ART resistant parasites compared with sensitive parasites (13, 16, 54–59) and some of these might correspond to such changes in the background that alter the effect of K13 mutations, although some of these changes likely also are downstream effects of the resistance mechanism (30). The data presented here originates from a set of isogenic 3D7 parasites which differ only in the mutations studied. While this limits how confidently conclusions can be extrapolated to other parasite strains, it presents the advantage of separating effects caused by the studied mutations from effects of the genetic background. Due to its long presence in culture, 3D7 also avoids variations that may arise in more recently culture adapted lines that often show reduced growth levels and may still acquire further changes during continued culture to adapt for better growth in culture.

k13 E252Q was previously observed to inflict a fitness cost that is smaller than that of *k13* C580Y, however, these experiments were not performed using parasites with isogenic backgrounds (47). Our results confirm this finding in an isogenic background. It should also be noted that the long duration of the competition experiments may permit the $K13^{C580Y}$-29^{th} to revert back to a state similar to the $K13^{C580Y}$ parasites, as the continuous RSA selection pressure was lifted in the competition assay.

We observed a disproportionally high fitness cost in parasites with the *ubp1* mutation conferring ART resistance. This is in agreement with the finding that lowering endocytosis by conditional inactivation or disruption of K13 compartment proteins impairs parasite growth (7). The small fitness cost of *k13* mutations compared to other K13-compartment proteins is likely due to its role in endocytosis in rings only (7). Our findings therefore highlight the unique property of K13 whereas resistance-conferring changes in KICs also affect endocytosis in later stage parasites, incurring a higher fitness cost and this is a likely reason why *k13* is the predominant gene mutated to cause ART resistance. Due to their high fitness cost, changes outside *k13* are less likely to arise and the resistance level, as observed with the few found in the field (50, 60, 61), is low.

A combination of the *ubp1* mutation, with C580Y in *k13*, did not lead to additive or synergistic resistance. The same was true in a recent study for coronin R100K and E107V combined with *k13* C580Y (11). Together with the high fitness cost of changes outside K13 indicated by this and previous work (7), it therefore at present does not seem likely that such combinations will lead to hyper-resistant parasites in the field.

Double mutations in *k13* could be envisaged to result in a less costly change for parasite fitness. However, surprisingly neither the combination of a *k13* mutation with moderate and one with high resistance nor two that each cause high resistance, increased resistance and were not even additive. This finding was consistent with similar protein levels of the double mutated *k13* to the single mutated version, indicating that at least in these combinations, multiple mutations do not further destabilize K13.

Taken together the findings in this work indicate that hyper-resistant parasites are not likely to arise with the K13-based mechanism unless the trade-off between nutrient acquisition and ART resistance (7, 30) is circumvented by other means. The repertoire of possible *k13* mutations resulting in different levels of the protein in the cell may provide the parasite with the option to adapt to the optimal fitness and resistance for a given endemic setting and this may explain why low and high transmission regions differ in the mutations observed.

Materials and Methods

Plasmid construction

The N-terminal SLI plasmid of K13, pSLI-N-GFP-2xFKBP-K13-loxP (40) was modified for the Kelch13 mutant parasites as follows: the V520A mutation was obtained by amplifying the codon-changed synthesized version of *k13* with primers Kelch13_codon_ad_fw and K13(V520A)_mutant_rv, as well as K13(V520A)_mutant_fw and Kelch_codon_adjust_rv (all primers listed in Table S2). For the V589I mutation the primers Kelch13_codon_ad_fw and K13(V589I)_mutant_rv, as well as K13(V589I)_mutant_fw and Kelch_codon_adjust_rv and for the E612K mutation the primers Kelch13_codon_ad_fw and K13(E612K)_mutant_rv, as well as K13(E612K)_mutant_fw and Kelch_codon_adjust_rv were used. The respective two fragments were cloned into the pSLI-N-GFP-2xFKBP-K13-loxP via AvrII/StuI, resulting in the plasmid pSLI-N-GFP-2xFKBP-K13(V520A)-loxP, pSLI-N-GFP-2xFKBP-K13(V589I)-loxP and pSLI-N-GFP-2xFKBP-K13(E612K)-loxP.

For the mutation pool candidates the pSLI-TGD plasmid (40) was used. The homology region was directly linked to a synthesized functional codon-changed version of the corresponding candidate containing all selected mutations (Genscript). The fragments of the homology region and the mutated recodonized sequence of all candidates were cloned by Gibson assembly into the pSLI-TGD vector via NotI/MluI, resulting in the vectors pSLI-KIC1mutpool, pSLI-KIC2mutpool, pSLI-KIC4mutpool, pSLI-KIC5mutpool, pSLI-KIC7mutpool, pSLI-KIC9mutpool, pSLI-UBP1mutpool and pSLI-MyosinFmutpool. Sequencing was performed to confirm absence of undesired mutations.

To generate K13$^{V520A+C580Y}$, pSLI-N-GFP-2xFKBP-K13-loxP (40) was modified by amplifying *k13* from this plasmid using primers HB21, HB09, HB10 and HB02 to introduce the mutation encoding V520A and ligating the resulting fragment into the same vector at the AvrII/XhoI sites.

K13$^{R539T+C580Y}$ was generated as above with primers HB21, HB80, HB81 and HB02. The *ubp1* R3138H mutation was introduced into K13^{C580Y} parasites using a SLI2a plasmid based on the pSLI-3xHA plasmid (40) but containing yDHODH and BSD genes instead of Neomycin resistance gene and hDHFR respectively (62). The homology region was excised from the previously published *ubp1* R3138H plasmid (7) and ligated into the target plasmid using NotI and SalI. KIC4-TGD and KIC5-TGD plasmids were created by inserting the respective homology regions (7) into SLI2a plasmids (62).

Parasite culturing and transfection

P. falciparum 3D7 parasites (63) were cultivated at 37°C in 0+ erythrocytes in RPMI complete medium with 0.5% Albumax (Life Technologies) with 5% hematocrit and transfected as previously described (64, 65). Transgenic parasites were selected using 4 nM WR99210 (Jacobus Pharmaceuticals) or 2.5 µg-ml BSD (Invitrogen). For selection-linked integration, parasites were selected as previously described using 0.9 µM DSM1 (BEI resources) or 400 µg/ml G418 (Merck) (40). Correct integration was confirmed by PCR as described (40).

***In-vitro* ring-stage survival assay^{0-3h} (RSA) and consecutive RSAs**

All RSAs were performed according to the standard procedure described previously (42). 0-3 h old rings were treated with 700 nM DHA for 6 h and cultivated for another 66 h at 37°C. Giemsa smears were taken and parasite survival rate determined by comparing the parasitemia of viable parasites after DHA against the parasitemia of the untreated control. Parasites were defined as resistant when mean survival rate exceeded the cut-off value of 1% (42).

For the consecutive RSA, K13^{C580Y} parasites (7) were used. 66 h after the DHA pulse, Giemsa smears were taken and the surviving parasites of the DHA treated sample were re-cultivated in a new Petri dish. After sufficient parasitemia was reached, the parasites originating from the RSA survivors were subjected to a new RSA. This procedure was continuously repeated for 30 rounds. The *k13* gene of the resulting parasites K13^{C580Y}-29th was sequenced and showed no changed compared to the starting cell line which harbored a recodonized *k13* with the C580Y mutation (7).

Fluorescence microscopy

Microscopy was performed as described earlier (66). A Zeiss Axio Imager M1 or M2 provided with a Hamamatsu Orca C4742-95 camera was used for imaging. Zeiss Plan-apochromat 63x or 100x oil immersion objectives with 1.4 numerical aperture were used. Images were edited using Corel Photo Paint X8 and brightness and intensity were adjusted. Images that were used for quantification were not adjusted for brightness and intensity.

Measurement of protein amount by fluorescence intensity

GFP-K13 parasites were synchronized two times using 5% sorbitol at intervals of two days. After the second sorbitol synchronization, the cell lines were cultivated at 37°C for 2 more hours and then GFP signal of the ring-stage parasites was detected by fluorescence microscopy using the 63x oil immersion objective. GFP-K13 WT parasites were always imaged alongside parasites carrying mutations and were used to normalize the signal of mutation-harboring parasites. Parasites were selected based on DIC and then exposed for 200 ms to image green fluorescence. Total intensity of the GFP signal in foci was measured and background signal subtracted using ImageJ (ImageJ2 2018, (67)).

Growth assessment

The parasitemia of a mixed-stage parasite culture was measured by flow cytometry (40) and based on this the parasitemia was adjusted to 0.05 to 0.1% parasitemia in 2.5% hematocrit. The parasitemia was then measured again by flow cytometry to determine the start parasitemia. These parasites were cultivated for 96 h and the medium was changed every 24 h. After 96 h parasitemia was measured again by flow cytometry and divided by the starting parasitemia to obtain the fold change in parasitemia.

Competition assay

Schizonts were isolated using 60% percoll purification, washed once with medium and cultured for 6 hours to allow invasion of merozoites into new red blood cells. Remaining schizonts were removed by a 10-min incubation in 5% sorbitol solution. The resulting 0-6 h old parasites were cultured at 37°C for 20-24 h after which the parasitemia was measured by flow cytometry (40). Based on the determined parasitemia, the mutant K13 cell lines were co-cultivated in a 1:1 ratio with 3D7 control in a 5 mL Petri dish. The proportion of GFP-positive parasites was assessed by fluorescence microscopy until one parasite line reached 95% of parasite proportion.

Statistical analysis and malaria incidence data

Unpaired t-tests were performed and Pearson's r calculated using GraphPad Prism 9.0.2. Linear regressions were fit to log transformed data (GraphPad Prism). All error bars shown are standard deviations. Malaria incidence data was downloaded from https://ghdx.healthdata.org/gbd-results-tool.

Acknowledgements

We thank Jacobus Pharmaceuticals for supplying WR99210. DSM1 (MRA-1161) was received from MR4/BEI Resources, NIAID, NIH. We thank Birgit Förster for sequencing and Ralf Krumpkamp for helpful discussions. This research made use of PlasmoDB.org. H.M.B. acknowledges funding by the Ortrud Mührer Fellowship of the Vereinigung der Freunde des Tropeninstituts Hamburg e.V.. This study was in part funded by the German Center for Infection Research (TTU03.806). TS acknowledges funding by the European Research Council (ERC, grant 101021493).

Author contributions

T.S., O.M.A and J.M. conceived the project. T.S. supervised research. S.Schm., H.M.B. and D.P. performed experiments. S.Schm. and H.M.B analyzed data and prepared figures. H.M.B. and T.S. wrote the manuscript draft. All authors approved the manuscript.

Competing interests

The authors declare no competing interests.

References

1. Institute for Health Metrics and Evaluation (IHME), Global Burden of Disease Collaborative Network. Global Burden of Disease Study 2019 (GBD 2019) Results. (2021).

2. World Health Organization, *World malaria report 2021* (2021).

3. World Health Organization, *Report on antimalarial drug efficacy, resistance and response: 10 years of surveillance (2010-2019)* (2020).

4. B. Witkowski, *et al.*, Novel phenotypic assays for the detection of artemisinin-resistant Plasmodium falciparum malaria in Cambodia: in-vitro and ex-vivo drug-response studies. *Lancet Infect Dis.* **13**, 1043–1049 (2013).

5. F. Ariey, *et al.*, A molecular marker of artemisinin-resistant Plasmodium falciparum malaria. *Nature* **505**, 50–55 (2014).

6. J. Straimer, *et al.*, K13-propeller mutations confer artemisinin resistance in Plasmodium falciparum clinical isolates. *Science.* **347**, 428–431 (2015).

7. J. Birnbaum, *et al.*, A Kelch13-defined endocytosis pathway mediates artemisinin resistance in malaria parasites. *Science.* **367**, 51–59 (2020).

8. N. V. Simwela, *et al.*, Experimentally Engineered Mutations in a Ubiquitin Hydrolase, UBP-1, Modulate In Vivo Susceptibility to Artemisinin and Chloroquine in Plasmodium berghei. *Antimicrob. Agents Chemother.* **64**, e02484-19 (2020).

9. R. C. Henrici, D. A. van Schalkwyk, C. J. Sutherland, Modification of pfap2µ and pfubp1 Markedly Reduces Ring- Stage Susceptibility of Plasmodium falciparum to Artemisinin In Vitro. *Antimicrob. Agents Chemother.* **64**, e01542-19 (2019).

10. A. R. Demas, *et al.*, Mutations in plasmodium falciparum actin-binding protein coronin confer reduced artemisinin susceptibility. *Proc. Natl. Acad. Sci. U. S. A.* **115**, 12799–12804 (2018).

11. A. I. Sharma, *et al.*, Genetic background and PfKelch13 affect artemisinin susceptibility of PfCoronin mutants in Plasmodium falciparum. *PLOS Genet.* **16**, e1009266 (2020).

12. T. Yang, *et al.*, Decreased K13 Abundance Reduces Hemoglobin Catabolism and Proteotoxic Stress, Underpinning Artemisinin Resistance. *Cell Rep.* **29**, 2917-2928.e5 (2019).

13. N. F. Gnädig, *et al.*, Insights into the intracellular localization, protein associations and artemisinin resistance properties of Plasmodium falciparum K13. *PLOS Pathog.* **16**, e1008482 (2020).

14. G. Siddiqui, A. Srivastava, A. S. Russell, D. J. Creek, Multi-omics based identification of specific biochemical changes associated with PfKelch13-mutant artemisinin-resistant plasmodium falciparum. *J. Infect. Dis.* **215**, 1435–1444 (2017).

15. R. Schumann, *et al.*, Protein abundance and folding rather than the redox state of Kelch13 determine the artemisinin susceptibility of Plasmodium falciparum. *Redox Biol.* **48**, 102177 (2021).

16. A. Xiong, *et al.*, K13-Mediated Reduced Susceptibility to Artemisinin in Plasmodium falciparum Is Overlaid on a Trait of Enhanced DNA Damage Repair. *Cell Rep.* **32**, 107996 (2020).

17. D. Ménard, *et al.*, A worldwide map of Plasmodium falciparum K13-propeller polymorphisms. *N. Engl. J. Med.* **374**, 2453–2464 (2016).

18. B. H. Stokes, *et al.*, Plasmodium falciparum K13 mutations in Africa and Asia impact artemisinin resistance and parasite fitness. *Elife* **10**, e66277 (2021).

19. R. Amato, *et al.*, Genomic epidemiology of artemisinin resistant malaria. *Elife* **5**, e08714 (2016).

20. O. Miotto, *et al.*, Genetic architecture of artemisinin-resistant Plasmodium falciparum. *Nat. Genet.* **47**, 226–234 (2015).

21. N. K. Kayiba, *et al.*, Spatial and molecular mapping of Pfkelch13 gene polymorphism in Africa in the era of emerging Plasmodium falciparum resistance to artemisinin: a systematic review. *Lancet Infect. Dis.* **21**, e82–e92 (2021).

22. L. Ndwiga, *et al.*, A review of the frequencies of Plasmodium falciparum Kelch 13 artemisinin resistance mutations in Africa. *Int. J. Parasitol. Drugs Drug Resist.* **16**, 155–161 (2021).

23. B. Balikagala, *et al.*, Evidence of Artemisinin-Resistant Malaria in Africa. *N. Engl. J. Med.* **385**, 1163–1171 (2021).

24. World Health Organization, "Artemisinin resistance and artemisinin-based combination therapy efficacy" (2019).

25. A. Uwimana, *et al.*, Emergence and clonal expansion of in vitro artemisinin-resistant Plasmodium falciparum kelch13 R561H mutant parasites in Rwanda. *Nat. Med.* **26**, 1602–1608 (2020).

26. A. Uwimana, *et al.*, Association of Plasmodium falciparum kelch13 R561H genotypes with delayed parasite clearance in Rwanda: an open-label, single-arm, multicentre, therapeutic efficacy study. *Lancet Infect. Dis.* **21**, 1120–1128 (2021).

27. K. G.-P. S. WWARN, *et al.*, Clinical determinants of early parasitological response to ACTs in African patients with uncomplicated falciparum malaria: a literature review and meta-analysis of individual patient data. *BMC Med.* **13**, 212 (2015).

28. N. Scott, *et al.*, Implications of population-level immunity for the emergence of artemisinin-resistant malaria: a mathematical model. *Malar. J.* **17**, 279 (2018).

29. E. Y. Klein, D. L. Smith, R. Laxminarayan, S. Levin, Superinfection and the evolution of resistance to antimalarial drugs. *Proc. R. Soc. B Biol. Sci.* **279**, 3834–3842 (2012).

30. P. Mesén-Ramírez, *et al.*, The parasitophorous vacuole nutrient channel is critical for drug access in malaria parasites and modulates the artemisinin resistance fitness cost. *Cell Host Microbe* **29**, 1774-1787.e9 (2021).

31. S. Nair, *et al.*, Fitness Costs and the Rapid Spread of kelch13 -C580Y Substitutions Conferring Artemisinin Resistance. *Antimicrob. Agents Chemother.* **62**, e00605-18 (2018).

32. S. M. Taylor, *et al.*, Absence of putative artemisinin resistance mutations among Plasmodium falciparum in sub-Saharan Africa: A molecular epidemiologic study. *J. Infect. Dis.* **211**, 680–688 (2015).

33. A. Ouattara, *et al.*, Polymorphisms in the K13-propeller gene in artemisinin-susceptible Plasmodium falciparum parasites from Bougoula-Hameau and Bandiagara, Mali. *Am. J. Trop. Med. Hyg.* **92**, 1202–1206 (2015).

34. P. C. Bull, K. Marsh, The role of antibodies to Plasmodium falciparum-infected-erythrocyte surface antigens in naturally acquired immunity to malaria. *Trends Microbiol.* **10**, 55–58 (2002).

35. P. J. Rosenthal, The interplay between drug resistance and fitness in malaria parasites. *Mol. Microbiol.* **89**, 1025–1038 (2013).

36. F. J. I. Fowkes, P. Boeuf, J. G. Beeson, Immunity to malaria in an era of declining malaria

transmission. *Parasitology* **143**, 139–153 (2016).

37. WWARN K13 Genotype-Phenotype Study Group, Association of mutations in the Plasmodium falciparum Kelch13 gene (Pf3D7_1343700) with parasite clearance rates after artemisinin-based treatments—a WWARN individual patient data meta-analysis. *BMC Med.* **17**, 1 (2019).

38. B. Hogan, *et al.*, Malaria Coinfections in Febrile Pediatric Inpatients: A Hospital-Based Study from Ghana. *Clin. Infect. Dis.* **66**, 1838–1845 (2018).

39. MalariaGEN, MalariaGen (2021) (March 23, 2022).

40. J. Birnbaum, *et al.*, A genetic system to study Plasmodium falciparum protein function. *Nat. Methods* **14**, 450–456 (2017).

41. C. E. Eboumbou Moukoko, *et al.*, K-13 propeller gene polymorphisms isolated between 2014 and 2017 from Cameroonian Plasmodium falciparum malaria patients. *PLoS One* **14**, e0221895 (2019).

42. B. Witkowski, *et al.*, Novel phenotypic assays for the detection of artemisinin- resistant Plasmodium falciparum malaria in Cambodia: in-vitro and ex-vivo drug-response studies. *Lancet Infect Dis.* **13**, 1043–1049 (2013).

43. H. M. Behrens, S. Schmidt, T. Spielmann, The newly discovered role of endocytosis in artemisinin resistance. *Med. Res. Rev.* **41**, 2998–3022 (2021).

44. L. Paloque, *et al.*, Mutation in the Plasmodium falciparum BTB/POZ Domain of K13 Protein Confers Artemisinin Resistance. *Antimicrob. Agents Chemother.* **66**, e0132021 (2022).

45. M. Bushman, R. Antia, V. Udhayakumar, J. C. de Roode, Within-host competition can delay evolution of drug resistance in malaria. *PLOS Biol.* **16**, e2005712 (2018).

46. M. Legros, S. Bonhoeffer, A combined within-host and between-hosts modelling framework for the evolution of resistance to antimalarial drugs. *J. R. Soc. Interface* **13**, 20160148 (2016).

47. A. R. Tirrell, *et al.*, Pairwise growth competitions identify relative fitness relationships among artemisinin resistant Plasmodium falciparum field isolates. *Malar. J.* **18**, 295 (2019).

48. WWARN, Artemisinin Molecular Surveyor.

49. Institute for Health Metrics and Evaluation (IHME), Burden of Disease, Global Health Data exchange.

50. G. C. Cerqueira, *et al.*, Longitudinal genomic surveillance of Plasmodium falciparum malaria parasites reveals complex genomic architecture of emerging artemisinin resistance. *Genome Biol.* **18**, 78 (2017).

51. Y. D. Ndiaye, *et al.*, Genetic surveillance for monitoring the impact of drug use on Plasmodium falciparum populations. *Int. J. Parasitol. Drugs Drug Resist.* **17**, 12–22 (2021).

52. D. Menard, A. Dondorp, Antimalarial Drug Resistance: A Threat to Malaria Elimination. *Cold Spring Harb. Perspect. Med.* **7**, a025619 (2017).

53. J. Straimer, *et al.*, Plasmodium falciparum K13 Mutations Differentially Impact Ozonide Susceptibility and Parasite Fitness In Vitro. *MBio* **8**, e00172-17 (2017).

54. S. Mok, *et al.*, Artemisinin-resistant K13 mutations rewire Plasmodium falciparum's intra-erythrocytic metabolic program to enhance survival. *Nat. Commun.* **12**, 530 (2021).

55. S. Mok, *et al.*, Population transcriptomics of human malaria parasites reveals the mechanism of artemisinin resistance. *Science.* **347**, 431–435 (2015).

56. C. Dogovski, *et al.*, Targeting the Cell Stress Response of Plasmodium falciparum to Overcome Artemisinin Resistance. *PLOS Biol.* **13**, e1002132 (2015).

57. S. Bhattacharjee, *et al.*, Remodeling of the malaria parasite and host human red cell by vesicle amplification that induces artemisinin resistance. *Blood* **131**, 1234–1247 (2018).

58. M. Zhang, *et al.*, Inhibiting the Plasmodium eIF2α Kinase PK4 Prevents Artemisinin-Induced Latency. *Cell Host Microbe* **22**, 766–776 (2017).

59. J. Gibbons, *et al.*, Altered expression of K13 disrupts DNA replication and repair in Plasmodium falciparum. *BMC Genomics* **19**, 849 (2018).

60. S. Borrmann, *et al.*, Genome-wide screen identifies new candidate genes associated with artemisinin susceptibility in Plasmodium falciparum in Kenya. *Sci. Rep.* **3**, 3318 (2013).

61. G. Henriques, *et al.*, Directional selection at the pfmdr1, pfcrt, pfubp1, and pfap2mu loci of Plasmodium falciparum in Kenyan children treated with ACT. *J. Infect. Dis.* **210**, 2001–2008 (2014).

62. A. B. Soares, *et al.*, An unusual trafficking domain in MSRP6 defines a complex needed for Maurer's clefts anchoring and maintenance in P. falciparum infected red blood cells. *bioRxiv [Preprint]*, 2021.12.03.471078 (2021).

63. D. Walliker, *et al.*, Genetic analysis of the human malaria parasite Plasmodium falciparum. *Science.* **236**, 1661–1666 (1987).

64. W. Trager, J. Jensen, Human malaria parasites in continuous culture. *Science.* **193**, 673–675 (1976).

65. R. W. Moon, *et al.*, Adaptation of the genetically tractable malaria pathogen Plasmodium knowlesi to continuous culture in human erythrocytes. *Proc. Natl. Acad. Sci.* **110**, 531–536 (2013).

66. C. Grüring, *et al.*, Development and host cell modifications of Plasmodium falciparum blood stages in four dimensions. *Nat. Commun.* **2**, 165 (2011).

67. C. A. Schneider, W. S. Rasband, K. W. Eliceiri, NIH Image to ImageJ: 25 years of image analysis. *Nat. Methods* **9**, 671–675 (2012).